HHS Public Access

Author manuscript

ACS Appl Bio Mater. Author manuscript; available in PMC 2020 January 22.

Published in final edited form as:

ACS Appl Bio Mater. 2019 January 22; 2(1): 81–92. doi:10.1021/acsabm.8b00390.

Characterization of the Kinetics and Mechanism of Degradation of Human Mesenchymal Stem Cell-Laden Poly(ethylene glycol) Hydrogels

Michelle S. Mazzeo[†], **Tiffanie Chai**[‡], **Maryam Daviran**[‡], **Kelly M. Schultz**[*,‡]

[†]Department of Bioengineering, Lehigh University, Bethlehem, Pennsylvania 18015, United States

[‡]Department of Chemical and Biomolecular Engineering, Lehigh University, Bethlehem, Pennsylvania 18015, United States

Abstract

Human mesenchymal stem cells (hMSCs) are motile cells that migrate from their native niche to wounded sites where they regulate inflammation during healing. New materials are being developed as hMSC delivery platforms to enhance wound healing. To act as an effective wound healing material, the hydrogel must degrade at the same rate as tissue regeneration, while maintaining a high cell viability. This work determines the kinetics and mechanism of cell-mediated degradation in hMSC-laden poly(ethylene glycol) (PEG) hydrogels. We use a well-established hydrogel scaffold that is composed of a backbone of four-arm star PEG functionalized with norbornene that is cross-linked with a matrix metalloproteinase (MMP) degradable peptide. This peptide sequence is cleaved by cell-secreted MMPs, which allow hMSCs to actively degrade the hydrogel during motility. Three mechanisms of degradation are characterized: hydrolytic, noncellular enzymatic and cell-mediated degradation. We use bulk rheology to characterize hydrogel material properties and quantify degradation throughout the entire reaction. Hydrolysis and noncellular enzymatic degradation are first characterized in hydrogels without hMSCs, and follow first-order and Michaelis–Menten kinetics, respectively. A high cell viability is measured in hMSC-laden hydrogels, even after shearing on the rheometer. After confirming hMSC viability, bulk rheology characterizes cell-mediated degradation. When comparing cell-mediated degradation to noncellular degradation mechanisms, cell-mediated degradation is dominated by enzymatic degradation. This indicates hydrogels with hMSCs are degraded primarily due to cell-secreted MMPs and very little network structure is lost due to hydrolysis. Modeling cell-mediated degradation provides an estimate of the initial concentration of MMPs secreted by hMSCs. By

[*]**Corresponding Author** kes513@lehigh.edu. Tel: +1-610-758-2012.

Author Contributions

M.S.M. and K.M.S. designed the project. M.S.M., T.C., and K.M.S. performed the experiments and data analysis. M.S.M. and K.M.S. developed the model and wrote the manuscript. M.D. wrote and edited the manuscript.

Supporting Information

The Supporting Information is available free of charge on the ACS Publications website at DOI: 10.1021/acsabm.8b00390.

Hydrogel swelling, changes in the elastic and loss modulus, normalized elastic moduli, individual experiments of sheared viability for hMSC-laden hydrogels, and initial concentration of MMPs (PDF)

Notes

The authors declare no competing financial interest.

changing the concentration of hMSCs, we determine the initial MMP concentration increases with increasing hMSC concentration. This work characterizes the rate and mechanism of scaffold degradation, giving new insight into the design of these materials as implantable scaffolds.

Grapical Abstract

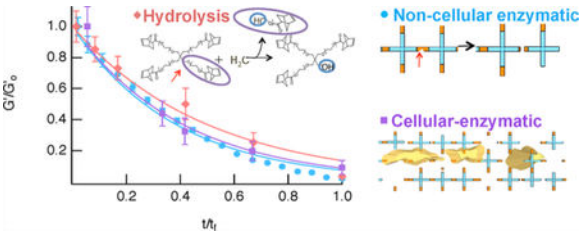

Keywords

hydrogel degradation; Michaelis–Menten kinetics; poly(ethylene glycol); hydrogels; cell motility; bulk rheology

INTRODUCTION

Hydrogel scaffolds have become an important class of biomaterials with applications in tissue regeneration, wound healing, and 3D cell culture.[1–15] These hydrogels can be composed of biologic or synthetic materials and are being designed as implantable scaffolds to enhance wound healing and tissue regeneration.[1–3,16–19] Within wound healing and regenerative medicine, these hydrogels are used to deliver drugs, proteins, or cells in vivo to specified locations within the body.[1,2,14,16,17,20] The encapsulation of human mesenchymal stem cells (hMSCs) is of particular interest because they are motile cells that naturally migrate from their native niche to wound sites to modulate inflammation, enhance the immune response, and help the healing process.[14,17,20–22] In order for types, including bone, cartilage, muscle, and adipose tissue, also plays an important role in tissue regeneration.[21,22] If implantable and degradable hydrogels can deliver additional hMSCs to a wound, the rate of wound healing and tissue regeneration can be increased. To do this, hydrogels must enable a high cell viability after encapsulation, provide structure to the tissue of interest, and degrade at the same rate as tissue regeneration.[6,25,26]

Poly(ethlyene glycol) (PEG)-based hydrogels have been used extensively as synthetic scaffolds for 3D cell encapsulation to determine the feasibility of these materials as implantable scaffolds.[1,5,8,9,12,16] PEG hydrogels are biocompatible and can be designed to mimic the stiffness of soft tissues, providing an environment that promotes basic cellular processes.[1,4] hMSCs to be motile, they secrete enzymes called matrix metalloproteinases (MMPs), which enable hMSCs to degrade the extracellular matrix and move through their microenviron-ment.[2,12,20,23,24] Their ability to differentiate into various cell Alternative materials include biologic hydrogels, which are scaffolds that incorporate components such as alginate, gelatin, and proteins, such as collagen. These materials are biodegradable and biocompatible.[1,18] However, there are advantages to using synthetic PEG hydrogels over biologic hydrogels. First, biologic hydrogels are weaker mechanically and more prone to

contamination.[27,28] Synthetic hydrogels have more controllable mechanical and chemical properties. They can also be tailored to cross-link with a wide range of chemistries and reaction schemes to form hydrogels within a wound site.[3,5] Unlike biologic hydrogels, synthetic PEG hydrogels can be designed to controllably present biological or physical cues to encapsulated hMSCs.[14,25,29] Biological scaffolds mimic the native extracellular matrix, including presentation of native physical and chemical cues that cannot be engineered.[30,31] Additionally, PEG hydrogels are hydrophilic, enabling them to absorb relatively large amounts of water-based media to maintain a high cell viability.[9] Their high mass transport capabilities and minimal protein adsorption make PEG hydrogels an excellent material for cell encapsulation.[16]

Due to the advantages of synthetic PEG hydrogels for cell encapsulation applications, we use PEG as the backbone for our scaffolds. In our hydrogel scaffold, multi-arm PEG is functionalized with norbornene anhydride to create endterminated PEG-norbornene molecules.[4,16] PEG is cross-linked with a MMP degradable cross-linker, KCGPQG↓IWGQCK. This cross-linker is chosen because it is degraded by hMSC-secreted MMPs during basic cellular processes.[6,14,16] Additionally, this cross-linker is degraded at a faster rate when compared to other MMP degradable peptide cross-linkers that better mimic collagen, because this sequence contains tryptophan instead of alanine.[6] This cross-linker is important for biomedical applications, since hydrogels that degrade more rapidly in vivo can lead to improved healing.[6] This scaffold is cross-linked using a photopolymerized step-growth reaction of thiols in the MMP degradable cross-linker and -enes in the norbornene. This reaction is used because it provides a relatively high mechanical integrity and allows for better spatial and temporal control of the hydrogel formed when compared to other step-growth reactions.[4,16]

After encapsulating hMSCs in our degradable PEG-norbornene (PEG-N) hydrogel, cell-mediated degradation is quantitatively characterized. It should be noted that during implantation, tissue will also provide cues to cells in the hydrogel that could increase MMP secretion and hMSC degradation of the scaffold.[20,32,33] Also, the tissue could provide additional MMPs that could potentially enhance scaffold degradation, beyond just enzymatic degradation from encapsulated hMSCs.[34,35] Our work begins by characterizing degradation in response to only cell-secreted enzymes and hydrolysis from the incubation environment. In our work, bulk rheology is used to measure the change in material properties of hMSC-laden hydrogels. These measurements determine the rate and mechanism of cell-mediated degradation. Rheology measures the deformation and flow of a material.[36] In our work, small amplitude oscillatory shear is used to measure the scaffold material properties. Bulk rheology characterizes the complex modulus of the material, $G^*(\omega)$, using

$$G^*(\omega) = G'(\omega) + iG''(\omega) \quad (1)$$

where ω is frequency, i is the unit imaginary number, G' is the storage or elastic modulus, and G'' is the viscous or loss modulus. Focusing primarily on G', these measurements characterize the material's elastic response and can be used to calculate gel stiffness.[37–39] Elastic modulus and stiffness are important parameters in cell motility and hydrogel

degradation.[11,18,40] In addition to bulk rheology, microrheology can also be used to characterize microenvironmental evolution around encapsulated cells.[12,41–44] Using microrheology, previous works have determined important information about cell-material interactions and how cells shape and degrade their hydrogel microenvironment.[10,12,45–48] However, minimal work has used bulk rheology to determine the material properties and degradation mechanisms during cellladen hydrogel degradation. Therefore, our work focuses on the rheological properties and degradation mechanisms of PEG-N hMSC-laden hydrogels by measuring their evolving elastic modulus, G', during scaffold degradation. These results can be combined with microrheological measurements to provide a more complete picture at the macroscopic and microscopic length scales.

Using bulk rheology, degradation mechanisms for hydrogels with hMSCs are characterized. Cell-mediated scaffold degradation is necessary for the survival of cells in the scaffold and can be manipulated by physical cues provided by the scaffold to enhance cell delivery during wound healing and tissue regeneration.[16,49] During motility, cells stretch, adhere, and degrade pathways through the scaffold. This cell-mediated degradation changes the material properties, scaffold structure, and kinetics of degradation.[10,40,47,50–52] In our hydrogel scaffold, degradation is the combination of hydrolysis and cell-mediated degradation, which occurs over different time scales. In order to understand the cell-mediated degradation rate, we must first characterize scaffold degradation by both mechanisms without cells.[6,7,12,18]

We use bulk rheology to characterize hydrogel degradation with and without hMSCs. The goal is to determine the kinetics and mechanism of hMSC-mediated hydrogel degradation. Hydrolytic and enzymatic degradation of the PEG-N scaffold without encapsulated hMSCs is characterized. Models are developed to describe both degradation mechanisms. Hydrolysis is modeled using first-order kinetics.[53,54] Michaelis– Menten kinetics are used to model enzymatic degradation. Hydrolytic and enzymatic kinetic constants are determined. Cell-mediated scaffold degradation is then characterized. A high hMSC viability is measured in these scaffolds prior to and after shear is applied during bulk rheological characterization. Hydrolytic and enzymatic models are fit to experimental data of cell-mediated degradation for hMSC-laden hydrogels. This determines the contributions of hydrolytic and cell-secreted enzymatic degradation in the overall hMSC-laden hydrogel degradation. Our work finds that cell-mediated degradation is dominated by cell-secreted enzymatic degradation and there is minimal hydrolytic degradation. By understanding how hMSCs degrade the pericellular region, hydrogels can be designed to more accurately manipulate cellular responses and the rate of scaffold degradation.[10,14,18,50] With knowledge of the hydrogel macroscopic material properties, combined with an understanding of how encapsulated hMSCs degrade hydrogels, these materials can be optimized for applications including implantable wound healing and tissue regeneration scaffolds. Although beyond the scope of this work, PEG-based hydrogels have shown promise in in vivo experiments as wound healing and tissue regeneration scaffolds.[55,56] Our work aims to determine the kinetics and mechanism of cell-mediated degradation for a well-defined PEG-peptide hydrogel. This work provides critical information that can be optimized in the design of new implantable tissue engineering or wound healing scaffolds.

EXPERIMENTAL SECTION

hMSC Culture.

hMSCs were purchased from Lonza in passage 2. Prior to receiving the hMSCs, Lonza was responsible for isolation of cells and the first passages. Frozen hMSCs were resuspended in 4 mL of growth medium, which consists of 1 g/L $_D$-glucose DMEM (Thermo Fisher Scientific), 10% fetal bovine serum (FBS, Thermo Fisher Scientific), 50 μmol mL^{-1} penicillin/streptomycin (Thermo Fisher Scientific), 0.5 μg mL^{-1} fungizone (Thermo Fisher Scientific), and 1 ng mL^{-1} recombinant human fibroblast growth factor (FGF, Peprotech, Inc.). FGF promotes hMSC proliferation and was added to the cell media to increase proliferation when culturing them prior to encapsulation.[57,58] This growth medium will be referred to as growth medium with FGF. hMSCs were pelleted and resuspended in 200–400 μL of growth medium with FGF[57,58] and were then added to a cell culture plate (150 mm × 25 mm Style Treated Cell Culture Dish, Corning Inc.) containing 40–60 mL of growth medium with FGF. This cell culture plate was incubated at 37 °C and 5% CO_2 (Galaxy 48R, New Brunswick Scientific Co., Inc.).[10,14] Growth medium with FGF was replenished after 3 days, which washes away any nonadherent hMSCs. After achieving 70–80% confluency, cells were either frozen in 95% 1 × Dulbecco's phosphate buffered saline (PBS, VWR Life Science) and 5% dimethyl sulfoxide (DMSO, Sigma-Aldrich Corporation) and returned to the –130 °C freezer and were passaged or remained in incubation for encapsulation. For passaging, 8 mL of a 0.25% trypsin–EDTA solution (Thermo Fisher Scientific) was added to the cell culture plate for 10–15 min to remove hMSCs from the bottom of the plate. Then 4 mL of growth medium with FGF was added to the cell culture plate, and all liquid was centrifuged for 5 min at 2600 rpm, resulting in a pellet of hMSCs. The liquid was decanted, and hMSCs were resuspended in 200–400 μL of PBS. hMSCs were then counted to determine the cell concentration from this passage. Cells were resuspended to the desired cell concentration during hydrogel fabrication, as discussed below. For all experiments, hMSCs were used in passage 2–6, and after passage 6, hMSCs were discarded.

Device Fabrication.

Hydrogels were made in custom sample chambers in a glass-bottomed Petri dish (d = 35 mm, no. 1.5 glass coverslip, MatTek Corporation). A polydimethylsiloxane (PDMS, Sylgard) cylindrical chamber with a 10 mm outer diameter and 8 mm inner diameter was made using biopsy punches (Integra Biosciences). The PDMS chamber was then loosely attached to the bottom of the glass-bottomed Petri dish using ultraviolet (UV) curing adhesive (Norland Optical Adhesive 81, Norland Products Inc.), which was cured with UV light at 365 nm for 3 min. This adhesive allows for sufficient attachment to the Petri dish but also allows for removal of the PDMS chamber. The PDMS chamber was used to hold the polymer precursor solution during the gelation process and was removed following gelation to enable equal swelling (in growth medium) in the axial and radial directions.

Hydrogel Fabrication.

Our hydrogel scaffold was composed of a four-arm star PEG-norbornene backbone (M_n = 20 000 g/mol, 3 mM, Sigma-Aldrich Corporation) cross-linked by a MMP degradable peptide, KCGPQG↓IWGQCK (M_n = 1305 g/mol, 3.9 mM, Bachem). This scaffold is well-

established for 3D cell encapsulation.[6,14] PEG-norbornene was purchased from Sigma-Aldrich as a powder. The linkage between the PEG molecule and the norbornene functionality is an ester. This ester linkage is the component of the molecule that hydrolyzes when the scaffold is incubated in water-based growth medium over the course of approximately 2 weeks. PEG-norbornene solutions were made by dissolving the PEG powder in a 1× phosphate buffered saline. In all of the experiments (cell-free and cell-laden), the same PEG-norbornene molecules were used. Hydrogels were photopolymerized with a thiol:ene stoichiometric ratio of 0.65.[4,12,16] A 0.65 thiol:ene ratio is a low cross-linking density, which results in a low modulus material.[14] In previous studies, this scaffold and cross-linking density has been shown to enable a high percentage of cells migrating within the hydrogel.[14] As discussed previously, since PEG-N scaffolds provide no physical or chemical cues in the environment, an adhesion ligand CRGDS (M_n 594 g/mol, 1 mM, American Peptide Company) was included to facilitate cell adhesion to the hydrogel.[16] Lithium phenyl-2,4,6-trimethylbenzoylphosphate (LAP, 1.7 mM), a photoinitiatior synthesized using previously published protocols was included to initiate the reaction.[59]

For scaffolds without hMSCs, the polymer precursor solution is described above. For hMSC-laden hydrogels, hMSCs were added to the polymer precursor solution prior to gelation and were encapsulated at a final concentration of 2×10^5 cells/mL. Note that this low cell concentration was used to limit cell–cell interactions within the hydrogel, so that we measure only cell-material interactions.[10,14] For all scaffolds, 100 μL of a polymer precursor solution was pipetted into the 8 mm sample chamber described above. The solution was exposed to UV light (365 nm, Analytik Jena US) for 3 min to initiate gelation. A cross-linked network forms through a radically mediated thiol:ene step-growth mechanism. Previous work has shown that UV exposure leads to successful 3D cell encapsulation and does not damage or kill the majority of hMSCs.[4,59] After gelation, the PDMS chamber was removed from the sample chamber to allow the gel to swell isotropically. The hydrogel was incubated in 3 mL of growth medium without FGF at 37 °C and 5% CO_2. FGF was not included in this media because it promotes cell proliferation. The focus of this work is motility, and this media was used to limit proliferation in our experiments.[14,57,58]

Hydrogel Degradation.

Three types of hydrogel degradation were characterized: hydrolytic, noncellular enzymatic, and cell-mediated degradation. In hydrolysis, the ester linkage in PEG molecules was hydrolyzed.[53] This occurs when the scaffold was incubated in water-based growth medium and results in degradation of hydrogels over the course of approximately 2 weeks.[53,60] For these experiments, hydrogels were incubated in growth medium without FGF at 37 °C and 5% CO_2 throughout the entire degradation reaction.[14] They were only removed immediately before characterization on the bulk rheometer. On the rheometer, hydrogels were incubated in an immersion cup (TA Instruments) filled with 6 mL of growth medium without FGF at 37 °C.

Noncellular enzymatic degradation was initiated by incubating hydrogels without hMSCs in a solution of collagenase (Sigma-Aldrich). Collagenase is a mixture of enzymes secreted by *Clostridium histolyticum*, with products identified by the relative ratios of the 10–18

components found in the secreted enzymes. The main components are two collagenases, clostripain, and a neutral protease.[61] The activity of our collagenase is 0.25–1.0 FALGPA units/mg solid, ≤125 CDU/ mg solid. One collagen digestion unit (CDU) removes peptides from collagen from bovine achilles tendon equivalent in ninhydrin color to 1.0 μmol of leucine in 5 h at pH 7.4 at 37 °C in the presence of calcium ions. One FALGPA hydrolysis unit hydrolyzes 1.0 μmol of furylacryloyl-Leu-Gly-Pro-Ala per min at 25 °C.[61] The enzymes cleave the MMP degradable cross-linker in the hydrogel, resulting in degradation. In our experiments, we used a 0.3 mg/mL collagenase solution. For these experiments, hydrogels were incubated in an immersion cup filled with 6 mL of collagenase at 37 °C on the rheometer. The elastic moduli was measured at timed intervals over the entire degradation reaction.

Cell-mediated degradation was measured in hMSC-laden hydrogel scaffolds. For these experiments, hMSCs were encapsulated in the hydrogel, which were incubated in growth medium without FGF. Following encapsulation, hMSCs secrete MMPs that degrade the MMP degradable cross-linker within the gel.[10,14,29] This degradation allows hMSCs to shape their environment in order to move through the hydrogel. For these experiments, hydrogels were kept in the incubator until running the scaffold on the rheometer. On the rheometer, hydrogels were incubated in an immersion cup filled with 6 mL of growth medium without FGF at 37 °C. Rheological measurements characterize hydrogel degradation over the five day degradation period.

Bulk Rheology.

Prior to bulk rheology measurements, Petri dish sample chambers were removed from the incubator, and growth medium without FGF was removed from the inside of the Petri dish. The hydrogel was removed from the sample chamber. The hydrogel was then cut using an 8 mm biopsy punch to ensure the hydrogel diameter matches the diameter of the geometry. Rheological properties were measured with a bulk rheometer (Ares G2, TA Instruments) using an 8 mm parallel plate, which is sandblasted to minimize slip. All hydrogels were incubated during measurements. An immersion cup was fixed to the Peltier plate and filled with 6 mL of solution. For hydrolysis and cell-mediated degradation, the hydrogels were incubated in growth medium without FGF at 37 °C. This provides hMSC-laden hydrogels with a growth medium during bulk rheology experiments. Noncellular enzymatic hydrogels were incubated in 6 mL of collagenase during bulk rheological measurements. A frequency sweep from 0.1 to 40 Hz at 1% strain was used to measure the moduli in each hydrogel sample.

Cell Viability.

To assess hMSC viability, a Live/Dead Viability Assay Kit (Thermo Fisher Scientific) was used to differentiate live and dead cells based on the integrity of the cell membranes.[13] The green-fluorescent calcein-AM highlights intracellular esterase activity found in live cells, while the red-fluorescent ethidium homodimer-1 enters the degraded plasma membrane found in dead cells.[62] Viability tests were completed by removing all growth medium from the sample chamber and pipetting 1 mL of the Live/Dead Viability Assay solution directly onto the hydrogel. The solution was left on the hydrogel for 30–60 min as per the

manufacturers instructions. An incubation time of 60 min was used to ensure that the assay could diffuse through the hydrogel scaffold. The scaffold was then imaged on an inverted fluorescent microscope (Axio Observer Z1, Carl Zeiss AG) using a 10× objective to capture images of red and green staining. Quantitative analysis was completed in ImageJ (NIH Image) by counting live and dead cells.

RESULTS AND DISCUSSION

The overall goal of this work is to characterize scaffold degradation to determine the cell-mediated degradation rate and mechanism. By identifying the cell-mediated degradation mechanism, hydrogels can be optimized for future use as wound healing and tissue regeneration scaffolds. In order to determine the overall mechanism of cell-mediated degradation, we first characterize degradation of hydrogels without hMSCs by hydrolytic and enzymatic degradation. These degradation mechanisms are compared to cell-mediated degradation to determine how both degradation mechanisms contribute to cell-mediated degradation. In addition to characterizing cell-mediated degradation, our experiments show hMSCs are viable within these hydrogels, even after experiencing stress. Our measurements determine that enzymatic degradation dominates the cell-mediated degradation mechanism, indicating cell-secreted enzymes are primarily responsible for hMSC-laden hydrogel degradation.

Hydrolytic Scaffold Degradation.

Hydrogels without decrease in the elastic moduli over the swelling period, the first 4 h of incubation in growth medium, until the moduli becomes constant and the scaffold is fully swollen. Since measuring the elastic moduli is also the primary method for tracking hydrogel degradation, it is important to use the swollen modulus as the initial modulus, G'_0. Therefore, a 4 h time point, after swelling is complete, is included in all experiments and used as the initial elastic modulus. Additional information regarding hydrogel swelling is provided in Figures S1 and S2.

Bulk rheological measurements characterize hydrolytic hydrogel degradation, quantifying the change in elastic moduli, G'. The value of G' is directly related to the cross-link density of the scaffold, ρ, making this a quantitative measure of the decrease in cross-links in our hydrogel scaffold. Hydrogels without cells degrade by hydrolysis of the ester linkage in the PEG molecules, which occurs during incubation in water-based growth medium.[53,60] As seen in Figure 1a, the elastic modulus is measured as a function of time over the course of the hydrogel degradation reaction. Complete degradation takes approximately 2 weeks. In Figure 1b, the elastic moduli is normalized by the initial elastic moduli, G'_0, and modeled. Hydrolysis follows first-order reaction kinetics[53] and is modeled by

$$\frac{G'}{G'_0} = e^{-k_h t} \quad (2)$$

where k_h is the hydrolysis kinetic constant and t is time. This results in a hydrolysis kinetic constant of $7.5 \times 10^{-3} \pm 7.1 \times 10^{-4}$ h^{-1}. This value agrees with literature values, which range from 2.1×10^{-2} h^{-1} to 4.2×10^{-4} for similar hydrogel chemistries.[8,54,63,64] Additional hydrolysis experiments and modeling are included in Figure S3.

Noncellular Enzymatic Scaffold Degradation.

Prior to measuring cell-mediated scaffold degradation, enzymatic degradation of our hydrogel scaffold is characterized. Collagenase is used as a control to validate the Michaelis– Menten enzymatic degradation model derived here. Collagenase has been used previously as a mimic for some of the protease that are secreted by hMSCs.[12,65,66] These studies use collagenase as a control to mimic enzymatic degradation, although the concentration of the enzymes will not be the same as the concentration secreted by hMSCs, the degradation mechanism will be the same.

Degradation is initiated by immersing the hydrogel in a 0.3 mg/mL collagenase solution. Before cell encapsulation, collagenase is used to homogeneously degrade the scaffold to study noncellular enzymatic degradation.[12] Hydrogels are incubated in a collagenase solution for 3.5 h. The maximum mesh size of the scaffold is approximately 10 nm, and a collagenase molecule is an order of magnitude smaller.[12,67] This indicates that collagenase will have unhindered diffusion into the scaffold. Figure 2a is bulk rheology of noncellular enzymatic scaffold degradation. The elastic moduli decrease with time, which occurs on a much faster time scale when compared to hydrolytic degradation. Note that since the time of degradation is a function of the collagenase concentration, changing the enzyme concentration can be used to vary the time of degradation. This has been measured in previous studies.[12] While lowering the enzyme concentration can lengthen the reaction, it is unlikely that it would lengthen the experiment to the two week period of hydrolysis.[12] We have also designed this experiment to happen on a fast time scale so that hydrolysis does not significantly contribute to the degradation reaction, and the experimental results characterize only enzymatic degradation.

Noncellular enzymatic degradation is modeled by taking into account cleavage of the MMP degradable cross-linker, deactivation of collagenase, and using material balances and Michaelis–Menten kinetics. For the cleavage of the MMP degradable cross-linker, this considers the probability, P, of a given cross-link being cleaved. The probability is quantified in eq 3, where $\frac{N_{\text{cross-link}}}{N_{\text{cross-link}_0}}$ is the normalized number of cross-links within the hydrogel, and G'/G'_0. is the normalized elastic moduli, at a given time. In this model, the normalized number of cross-links is equivalent to the normalized elastic moduli, G'/G'_0. The enzymatic kinetic constant, $k^* = \frac{k_{\text{cat}}}{K_m}$, is then determined from this model,

$$P = \frac{N_{\text{cross-link}}}{N_{\text{cross-link}_0}} = \frac{G'}{G'_0} = \mathrm{e}^{\frac{k^*[\text{collagenase}]_0}{k_d}(e^{-k_d t}-1)} \quad (3)$$

where $[\text{collagenase}]_0$ is the initial concentration of collagenase and k_d is the first-order rate constant.[7,12,63] The initial concentration of collagenase is equal to 2.31×10^{-6} M for our experiments. The deactivation of collagenase follows a first-order decay. Using the previously measured half-life of collagenase, ≈48 h, the first-order rate constant k_d is 0.02 h^{-1}.[7,12,19] Equation 3 is fit to the normalized elastic moduli data, Figure 2b, and results in an enzymatic kinetic constant of $k^* = 86.7 \pm 0.71\ M^{-1}\ s^{-1}$ ($k^*_{\text{normalized}} = 22\,000 \pm 180\ M^{-2}\ s^{-1}$). Our enzymatic kinetic constant falls within the literature range from 50 to 11 000 $M^{-1}\ s^{-1}$.[6] The wide range of values in the literature is because previous work measured the cleavage of this specific MMP degradable cross-linker sequence by single MMPs (MMP-1, MMP-2, MMP-3, MMP-8, or MMP-9).[6] Additional noncellular enzymatic degradation experiments and fits are included in Figure S4.

Bulk rheological measurements of noncellular enzymatic degradation are compared to previous microrheology measurements of noncellular enzymatic degradation in this material.[12,47] Previous multiple particle tracking microrheological characterization of this scaffold determines a value of k^* that falls within the range of enzymatic kinetic constants in the literature, 2100 $M^{-1}\ s^{-1}$.[6,12] In this work, a different collagenase concentration is used to degrade the hydrogel, possibly accounting for the variability of the rate constant.[12] To account for the differences in these experiments, both bulk rheological and previous microrheological measurements are normalized and plotted together in Figure 3. Each set of data is from a single degradation reaction measurement, but is representative data. The results are comparable over the entire degradation reaction regardless of measurement technique. Additionally, eq 3 accurately describes both sets of data.

Bulk rheological characterization of noncellular enzymatic degradation is also compared to hydrolytic degradation results. Time is normalized by the final time of degradation, t_f, as these experiments occur over different time scales. Hydrolysis takes approximately 2 weeks, while noncellular enzymatic degradation occurs over several hours. Comparing the measurements and resulting fits, Figure 4, the shape of the curves are essentially the same. This is a result of the moduli during both degradation reactions having an exponential decay which is described in the models, eqs 2 and 3. However, there are differences between the two sets of data, including a slower rate of change in the moduli during hydrolysis, even after normalization. This data indicates that the rate of loss of cross-links by enzymatic degradation is quicker than during hydrolytic degradation. This will result in not only an overall faster degradation reaction, but also a faster loss of cross-links in the initial stages of degradation when the scaffold is degraded enzymatically.

By characterizing hydrolytic and enzymatic degradation in hydrogel scaffolds without hMSCs, we measure the kinetics of scaffold degradation and use models to determine the

reaction constants. These experimental results and reaction constants are then compared to measurements of cell-mediated degradation.

Cell Viability.

Prior to bulk rheological characterization of cell-mediated degradation of hMSC-laden hydrogels, we must confirm that hMSCs remain viable during and after the measurement. Hydrogels with hMSCs are swollen in growth medium, and hydrogels are stained with a Live/Dead assay to determine temporal changes in cell viability. Live cells are stained green due to intracellular esterase activity, and dead cells are stained red due to lack of membrane integrity.[62] By counting the number of live and dead cells, we quantify hMSC viability for each hydrogel at various times throughout our experiments. Viability is first measured after only incubating cell-laden hydrogels at 37 °C and 5% CO_2 with no external forces applied. These experiments will be referred to as “incubation viability”. Incubation viability experiments collect data 4, 24, 48, and 120 h after hydrogel incubation. The resulting data, Figure 5, shows that incubation viability remains high with only a slight decrease in viability over time. Additionally, cell imaging shows that cells are motile within the hydrogel. Figure 5 also shows hMSC stretching increases over time. This motility is indicative of hMSC viability within the hydrogel, as hMSCs are motile cells that naturally migrate in their environment.[14,17,22] Since no change is measured in cell viability between 48 and 120 h, experiments are shortened and taken to 72 h for the remaining scaffolds.

Cell viability is determined after hMSC-laden hydrogels are sheared on the rheometer, which is referred to as “sheared viability”. For these experiments, hMSC-laden hydrogels are incubated immediately after gelation until they are measured on the rheometer, where they experience shear, and then viability is completed immediately after the bulk rheology experiment. For sheared viability experiments data are collected after 0, 24, 36, 48, and 72 h of incubation. Figure 5e,f is a quantification of cell viability, where time is the incubation time following gelation and prior to bulk rheological characterization. In Figure 5f, there is a slight decrease in viable cells after hMSC-laden hydrogels are sheared, but the sheared viability results are comparable and remain within error of incubation viability values. This indicates that hMSCs encapsulated in these hydrogels can survive bulk rheological measurements, and therefore, hMSCs can withstand stresses when encapsulated within these hydrogels. Additional information for sheared viability experiments is included in Figure S5.

Additionally, hMSC viability is monitored at several time points following bulk rheology measurements. These experiments determine if additional hMSC death occurs at later time points following the initial application of stress. In this experiment, hMSC-laden hydrogels have viability measured at 0, 24, or 48 h after shearing on the rheometer, Figure 6. Note that, in real time, all shearing occurs at 48 h and that viability measurements are completed at 48, 72, or 96 h after hydrogel gelation, respectively; 91 ± 10% of hMSCs are viable immediately (zero hours) after shearing. hMSC viability remains constant 24 and 48 h after shearing, with values of 87 ± 9.0% and 85 ± 8.0%, respectively, Figure 6. This indicates that minimal to no additional hMSC death occurs hours after hMSCs experience stress.

Since hMSCs encapsulated in the hydrogels are exposed to ambient conditions during bulk rheological characterization, additional viability testing is done to confirm that hMSC

viability does not decrease during these experiments. During incubation, CO_2 is absorbed into the growth medium and is expected to have a relatively quick desorption from the hydrogels. Our hydrogels are water-based, and previous work has determined that CO_2 desorption in water at physiological temperatures occur in 5–10 min.[68] Therefore, it can be assumed that there will be CO_2 desorption from hydrogels before the completion of a bulk rheology experiment.

Due to this, we measure viability in hydrogels with encapsulated hMSCs that are exposed to ambient conditions without growth medium for up to 30 min. These experiments are done without growth medium to create the harshest environmental change a hydrogel will experience. All bulk rheological measurements are taken in growth medium. This is referred to as “exposure viability”. Exposure viability results show no notable change in hMSC viability over a 30 min time period, Figure 7. Since each bulk rheology experiment only exposes the hMSC-laden hydrogels for about 15 min, it can be concluded that exposure to natural CO_2 conditions should not impact viability during bulk rheology experiments. These experiments show that any changes in hMSC viability is a result of the shear applied during bulk rheology experiments, rather than exposure to ambient conditions.

Cell-Mediated Degradation.

After hMSC viability is confirmed, bulk rheology characterizes cell-mediated hydrogel degradation. Figure 8a shows the decrease in modulus over time. In Figure 8a, the initial elastic moduli of hMSC-laden hydrogels are 5–6× less than hydrogels without hMSCs. The initial elastic moduli of hydrogels with hMSCs are likely lower due to encapsulated hMSCs taking up additional space within the hydrogel and preventing cross-linking. hMSCs are on the micrometer scale, and cross-links are on the nanometer scale, so the encapsulation of hMSCs prevents additional cross-links from forming. Therefore, the hydrogel will have fewer cross-links, resulting in a decrease in stiffness characterized by a lower initial elastic moduli. This can be verified by comparing the estimated number of cross-links lost in a hydrogel to the elastic moduli data for hydrogels with and without hMSCs.

In an ideal system where 100% of cross-links form, the maximum dimension of a pore in a hydrogel without hMSCs is approximately 10 nm. This is calculated assuming a square pore and using the contour length of a PEG arm as a side of the pore. When cells are added to the scaffold, they prevent formation of some of the cross-linkers by taking up space in the hydrogel. The average cell radius is 10 μm, and the cell volume is calculated by assuming they are spherical. Then the average volume taken up by cells is calculated by the spherical volume of a single cell multiplied by the number of cells in the scaffold. The maximum pore dimension is approximately 10 nm, which is the basis for the pore volume calculation. By dividing the volume taken up by the cells by the pore volume, we determine the change in average pore size. From this calculation, hMSC-laden hydrogels have an average maximum pore length of about 17 nm. When factoring in that cross-linking efficiency $\left(\frac{\rho_{\text{hydrogelwithoutMSCs}}}{\rho_{\text{idealsystem}}}\right)$ is 30% (determined from bulk rheological measurements), Table 1, 80% of cross-links is lost when hMSCs are encapsulated in a hydrogel.[69] This is compared to bulk rheology data, where swollen hydrogels with hMSCs have an elastic modulus of

about 100 Pa and swollen hydrogels without hMSCs are approximately 550 Pa. These measurements also determine that about 80% of cross-links are lost. We do this using the equation $G' \sim \rho k_b T$, where ρ is the crosslinks density, T is the temperature, and k_b is the Boltzmann constant. ρ is calculated from the measured moduli of swollen hydrogels with and without hMSCs. The percentage of crosslinks lost is calculated using $\frac{\rho_{\text{withouthMSCs}} - \rho_{\text{withhMSCs}}}{\rho_{\text{withouthMSCs}}}$.[69]

The normalized elastic moduli, G'/G'_0, is modeled to determine the degradation mechanism for hydrogels with encapsulated hMSCs. Cell-mediated hydrogel degradation is a combination of hydrolysis and cell-mediated enzymatic degradation. Data sets are fit to an enzymatic degradation model based on Michaelis–Menten kinetics that described the collagenase experiments. These experimental results were initially fit with hydrolytic, enzymatic, and a combination of hydrolytic and enzymatic degradation kinetic models. The only model that fit the data is an enzymatic degradation model, indicating that hMSC-mediated scaffold degradation is due to MMP degradation within the scaffold and hydrolysis accounts for minimal scaffold degradation. During these measurements, the hydrogel is degraded enzymatically by cell-secreted MMPs, rather than by a collagenase solution. Due to this, modifications are made, and the resulting equation describes cell-mediated degradation

$$\frac{G'}{G'_0} = e^{\frac{k^* [\text{MMP}]_0}{k_d}(e^{-k_d t} - 1)} \quad (4)$$

where the initial concentration of MMPs, $[\text{MMP}]_0$, is incorporated into the equation. Since collagenase is a solution of MMPs, the first-order rate constant, k_d, used in the previous enzymatic model, is used, and equals 0.02 h^{-1}. Additionally, the previously determined enzymatic kinetic constant, k^*, is used to account for enzymatic degradation, which equals 86.7 ± 0.71 M^{-1} s^{-1}.

Since the initial concentration of secreted MMPs is unknown, we use eq 4 to fit for $[\text{MMP}_0]$, which provides an approximation of the initial MMP concentration secreted by encapsulated hMSCs. This value is $1.52 \times 10^{-7} \pm 2.05 \times 10^{-8}$ M in a hydrogel with 2×10^5 cell/mL. Literature has confirmed the presence of specific MMPs and studies how MMPs can be used to regulate cell behavior, particularly involved with inflammation, tissue regeneration, and cancer cell applications.[34,48,70] However, no estimate of a cell-secreted MMP concentration appears in these works, especially when encapsulated in hydrogels.[34,48,70] This model gives an indirect estimate of MMPs secreted by hMSCs encapsulated within these hydrogels, which can be used to target a specific degradation rate when designing these materials. Therefore, additional knowledge about hMSC-secreted MMPs helps to increase the tailorability of these hydrogels in specific wound healing applications, by matching the rate of hydrogel degradation to the rate of tissue regeneration within a specific wound.

Experimental replicates and their corresponding initial MMP concentrations are included in Figure S6.

hMSC-laden hydrogels can also be tailored by varying the hMSC concentration within the hydrogel. All previous experiments encapsulated hMSCs in hydrogels at a concentration of 2×10^5 cells/mL. In order to determine how hMSC concentration affects cell-mediated degradation, bulk rheology experiments also characterize hydrogels with encapsulated hMSCs at concentrations of 0.5×10^5 and 1×10^5 cells/mL. Figure 9. Complete hydrogel degradation with a higher cell concentration (2×10^5 cells/mL) and lower cell concentration (0.5×10^5 and 1×10^5 cells/mL) happens after 72 and 96 h, respectively. This indicates that hydrogel degradation does constant. ρ is calculated from the measured moduli of swollen hydrogels with and without hMSCs. The percentage of cross-occur faster when a higher concentration of cells is encapsulated in the scaffold. These measurements determine that hydrogel degradation is faster when higher concentrations of cells are encapsulated in the scaffold. Elastic moduli data at each concentration is fit to eq 4, which fits for $[MMP]_0$, the initial concentration of MMPs secreted by hMSCs. From this, $[MMP]_0$ is found to be $1.04 \times 10^{-7} \pm 1.4 \times 10^{-8}$ M and $1.15 \times 10^{-7} \pm 1.3 \times 10^{-8}$ M for hMSC concentrations of 0.5×10^5 and 1×10^5 cells/mL, respectively. From this study, we estimate that as the concentration of hMSCs encapsulated within the hydrogels increases, the concentration of MMPs secreted by the cells also increases. This is an expected result, when more hMSCs are present, more MMPs are secreted that actively degrade the hydrogel to enable cell motility, which changes the rate of hydrogel degradation.

The change in $[MMP_0]$ is statistically significant between 1×10^5 and 2×10^5 cell/mL, but is within error for 0.5×10^5 and 1×10^5 cells/mL. The values being within error for the lower concentrations is not unexpected. In this low cell concentration, we expect a lower overall MMP secretion. Additionally, with the smaller change between the two lower hMSC concentrations, a smaller decrease in the change of $[MMP_0]$ is expected. This shows that altering the hMSC concentration provides another method to optimize cell-mediated hydrogel degradation rates for different wound healing and tissue regeneration applications. Additional information for how $[MMP_0]$ changes with hMSC concentration are included in Figure S7.

In Figure 10, all degradation reactions are plotted together. Since all of the previously discussed types of degradation occur on different time scales, all elastic modulus data are normalized, which enables direct comparison of all the degradation mechanisms. The hydrolytic degradation rate is slower than the noncellular enzymatic and cell-mediated degradation rates. Cell-secreted enzymes are degrading the hydrogel on a time scale much faster than hydrolysis, thereby minimizing effects from hydrolytic degradation. When comparing hydrolytic degradation (total degradation in 288 h) to cell-mediated degradation (total degradation in 72 h) without normalizing time, degradation of hydrogels with encapsulated hMSCs occurs at a rate approximately 4× faster than hydrolytic degradation. This indicates hydrolysis plays a minimal role in the overall cell-mediated degradation mechanism. As cells secrete MMPs, the MMP degradable cross-linker is cleaved, thus degrading the hydrogel at a faster rate when compared to hydrolysis alone. On the other hand, when comparing cell-mediated degradation to noncellular enzymatic degradation,

these fits are closely aligned, and nearly overlap. The initial collagenase and MMP concentration are an order of magnitude different, $[\text{collagenase}_0] \approx 2.3 \times 10^{-6}$ and $[\text{MMP}_0] \approx 1 \times 10^{-7}$ M, which accounts for deviations in degradation data. This indicates that cell-mediated degradation is dominated by an enzymatic degradation mechanism.

CONCLUSION

PEG-N hydrogel degradation is characterized to determine the mechanism of cell-mediated degradation. Bulk rheology is used to determine the kinetics of three types of degradation: hydrolytic, noncellular enzymatic, and cell-mediated degradation. Hydrolytic degradation occurs due to hydrolysis of the ester linkage in the PEG molecules when hydrogels are incubated in growth medium. These experiments result in a hydrolysis kinetic constant, $k_h = 7.5 \times 10^{-3} \pm 7.1 \times 10^{-4}$ h^{-1}. Noncellular enzymatic degradation is initiated by incubating hydrogels in a collagenase solution. This cleaves the MMP degradable cross-linker in the hydrogel and results in an enzymatic kinetic constant, $k^* = 86.7 \pm 0.71$ M^{-1} s^{-1}.

Prior to measuring the cell-mediated scaffold degradation, viability measurements show that these hydrogels maintain a high hMSC viability and provide an environment where hMSCs survive in the presence of stress from bulk rheological characterizations. Once a high hMSC viability is confirmed, bulk rheology is used to characterize cell-mediated hydrogel degradation when hMSCs are encapsulated in the hydrogel. By comparing material degradation in the presence of hMSCs to control experiments of hydrolytic and enzymatic degradation (both without encapsulated hMSCs), we determine that cell-mediated degradation is due to MMP secretion and that hydrolytic degradation is minimal. To model this reaction, the enzymatic degradation model developed for noncellular enzymatic degradation is modified. Constants from hydrolytic and noncellular enzymatic degradation are used to determine the initial concentration of MMPs in the scaffold. By changing the concentration of encapsulated hMSCs, we indirectly estimate that the amount of MMPs in the hydrogel increases with an increasing hMSC concentration.

This work provides important new information about cell-mediated degradation. Namely, the mechanism of scaffold degradation has a minimal contribution from hydrolysis and is due to enzymatic degradation by cell-secreted MMPs. This work also provides a method to estimate the initial concentration of MMPs present in a cell-laden hydrogel scaffold. These results characterize the evolving material Iproperties of these hydrogels throughout degradation, which can be used to optimize cell-laden hydrogels in future regenerative medicine and wound healing applications.

Supplementary Material

Refer to Web version on PubMed Central for supplementary material.

ACKNOWLEDGMENTS

The authors thank Dr. Matthew D. Wehrman for his support and helpful discussions.

Funding

Funding for this work was provided by the Lehigh University's Presidential Scholarship program (MSM) and the National Institute of General Medical Sciences of the National Institutes of Health under award no. R15GM119065. The content is solely the responsibility of the authors and does not necessarily represent the official views of the National Institutes of Health.

ABBREVIATIONS

hMSCs	human mesenchymal stem cells
PEG	poly(ethylene glycol)
PEG-N	poly(ethylene glycol)-norbornene hydrogel
MMP	matrix metalloproteinase
RGD	CRGDS
LAP	lithium phenyl-2,4,6-trimethylbenzoylphosphate
UV	ultraviolet
MPT	multiple particle tracking microrheology
FGF	fibroblast growth factor
PBS	phosphate buffered saline
PDMS	polydimethylsiloxane

REFERENCES

(1). Slaughter BV; Khurshid SS; Fisher OZ; Khademhosseini A; Peppas NA Hydrogels in Regenerative Medicine. Adv. Mater 2009, 21, 3307–3329. [PubMed: 20882499]

(2). Purcell BP; Lobb D; Charati MB; Dorsey SM; Wade RJ; Zellars KN; Doviak H; Pettaway S; Logdon CB; Shuman JA; Freels PD; Gorman JH III; Gorman RC; Spinale FG; Burdick JA Injectable and Bioresponsive Hydrogels for On-demand Matrix Metalloproteinase Inhibition. Nat. Mater 2014, 13, 653–661. [PubMed: 24681647]

(3). Place ES; George JH; Williams CK; Stevens MM Synthetic Polymer Scaffolds for Tissue Engineering. Chem. Soc. Rev 2009, 38, 1139–1151. [PubMed: 19421585]

(4). Fairbanks BD; Schwartz MP; Halevi AE; Nuttelman CR; Bowman CN; Anseth KS A Versatile Synthetic Extracellular Matrix Mimic via thiol-norbornene Photopolymerization. Adv. Mater 2009, 21, 5005–5010. [PubMed: 25377720]

(5). Zhu J Bioactive Modification of Poly(ethylene glycol) Hydrogels for Tissue Engineering. Biomaterials 2010, 31, 4639–4656. [PubMed: 20303169]

(6). Patterson J; Hubbell J Enhanced Proteolytic Degradation of Molecularly Engineered PEG Hydrogels in Response to MMP-1 and MMP-2. Biomaterials 2010, 31, 7836–7845. [PubMed: 20667588]

(7). Rice MA; Sanchez-Adams J; Anseth KS Exogenously Triggered, Enzymatic Degradation of Photopolymerized Hydrogels With Polycaprolactone Subunits: Experimental Observation and Modeling of Mass Loss Behavior. Biomacromolecules 2006, 7, 1968–1975. [PubMed: 16768421]

(8). Metters AT; Anseth KS; Bowman CN Fundamental Studies of a Novel, Biodegradable PEG-b-PLA Hydrogel. Polymer 2000, 41, 3993–4004.

(9). Chai Q; Jiao Y; Yu X Hydrogels for Biomedical Applications: Their Characteristics and the Mechanisms behind Them. Biomolecules 2013, 14, 949–953.

(10). Schultz KM; Kyburz KA; Anseth KS Measuring Dynamic Cell-material Interactions and Remodeling During 3D Human Mesenchymal Stem Cell Migration in Hydrogels. Proc. Natl. Acad. Sci. U. S. A 2015, 112, E3757–E3764. [PubMed: 26150508]

(11). Schultz KM; Furst EM Microrheology of Biomaterial Hydrogelators. Soft Matter 2012, 8, 6198–6205.

(12). Schultz KM; Anseth KS Monitoring Degradation of Matrix Metalloproteinases-cleavable PEG Hydrogels via Multiple Particle Tracking Microrheology. Soft Matter 2013, 9, 1570–1579.

(13). Alge DL; Azagarsamy MA; Donohue DF; Anseth KS Synthetically Tractable Click Hydrogels for Three-Dimensional Cell Culture Formed Using Tetrazine Norbornene Chemistry. Biomacromolecules 2013, 14, 949–953.

(14). Kyburz KA; Anseth KS Three-dimensional HMSC Motility within Peptide-Functionalized PEG-Based Hydrogel of Varying Adhesivity and Crosslinking Density. Acta Biomater 2013, 9, 6381–6392. [PubMed: 23376239]

(15). Peppas NA; Hilt JZ; Khademhosseini A; Langer R Hydrogels in Biology and Medicine: From Molecular Principles to Bionanotechnology. Adv. Mater 2006, 18, 1345–1360.

(16). Anderson SB; Lin C-C; Kuntzler DV; Anseth KS The Performance of Human Mesenchymal Stem Cells Encapsulated in Cell-degradable Polymer-peptide Hydrogels. Biomaterials 2011, 32, 3564–3574. [PubMed: 21334063]

(17). Ennis WJ; Sui A; Bartholomew A Stem Cells and Healing: Impact on Inflammation. Adv. Wound Care 2013, 2, 369–378.

(18). Brandl F; Sommer F; Goepferich A Rational Design of Hydrogels for Tissue Engineering: Impact of Physical Factors on Cell Behavior. Biomaterials 2007, 28, 134–146. [PubMed: 17011028]

(19). Mandl I; MacLennan JD; Howes EL; DeBellis R; Sohler A Isolation and Characterization of Proteinase and Collagenase from Cl. J. Clin. Invest 1953, 32, 1323–1329. [PubMed: 13109000]

(20). Ries C; Egea V; Karow M; Kolb H; Jochum M; Neth P MMP-2, MT1-MMP, and TIMP-2 are Essential for the Invasive Capacity of Human Mesenchymal Stem Cells: Differential Regulation by Inflammatory Cytokines. Blood 2007, 109, 4055–4063. [PubMed: 17197427]

(21). Mackenzie TC; Flake AW Human Mesenchymal Stem Cells Persist, Demonstrate Site-Specific Multipotential Differentiation and Are Present in Sites of Would Healing and Tissue Regeneration after Transplantation into Fetal Sheep. Blood Cells, Mol., Dis 2001, 27, 601–604. [PubMed: 11482873]

(22). Singer NG; Caplan AI Mesenchymal Stem Cells: Mechanisms of Inflammation. Annu. Rev. Pathol.: Mech. Dis 2011, 6, 457–478.

(23). Visse R; Nagase H Matrix Metalloproteinases and Tissue Inhibitors of Metalloproteinases: Structure, Function, and Biochemistry. Circ. Res 2003, 92, 827–839. [PubMed: 12730128]

(24). Lozito TP; Tuan RS Mesenchymal Stem Cells Inhibit Both Endogenous and Exogenous MMPs via Secreted TIMPs. J. Cell. Physiol 2011, 226, 385–396. [PubMed: 20665704]

(25). Benton JA; Fairbanks BD; Anseth KS Characterization of Valvular Interstitial Cell Function in Three Dimensional Matrix JMetalloproteinase Degradable PEG Hydrogels. Biomaterials 2009, 30, 6593–6660. [PubMed: 19747725]

(26). Lutolf MP; Lauer-Fields JL; Schmoekel HG; Metters AT; Weber FE; Fields GB; Hubbell JA Synthetic Matrix Metalloproteinase-sensitive Hydrogels for the Conduction of Tissue Regeneration: Engineering Cell-invasion Characteristics. Proc. Natl. Acad. Sci. U. S. A 2003, 100, 5413–5418. [PubMed: 12686696]

(27). Orban JM; Wilson LB; Kofroth JA; El-Kurdi MS; Maul TM; Vorp DA Crosslinking of Collagen Gels by Transglutaminase. J. Biomed. Mater. Res 2004, 68A, 756–762.

(28). Nerem R; Seliktar D Vascular Tissue Engineering. Annu. Rev. Biomed. Eng 2001, 3, 225–243. [PubMed: 11447063]

(29). Leight JL; Alge DL; Maier AJ; Anseth KS Direct Measurement of Matrix Metalloproteinase Activity in 3D Cellular Microenvironments Using a Fluorogenic Peptide Substrate. Biomaterials 2013, 34, 7344–7352. [PubMed: 23830581]

(30). Butcher JT; Nerem RM Porcine Aortic Valve Interstitial Cells in Three Dimensional Culture: Comparison of Phenotype with Aortic Smooth Muscle Cells. J. Heart Valve Dis 2004, 13, 478–486. [PubMed: 15222296]

(31). Eyrich D; Brandl F; Appel B; Wiese H; Maier G; Wenzel M; Staudenmaier R; Goepferich A; Blunk T Long-term Stable Fibrin Gels for Cartilage Engineering. Biomaterials 2007, 28, 55–65. [PubMed: 16962167]

(32). Phinney DG; Prockop DJ Concise Review: Mesenchymal Stem/Multipotent Stromal Cells: The State of Transdifferentiation and Modes of Tissue Repair - Current Views. Stem Cells 2007, 25, 2896–2902. [PubMed: 17901396]

(33). Lapidot T; Dar A; Kollet O How Do Stem Cells Find Their Way Home? Blood 2005, 106, 1901–1910. [PubMed: 15890683]

(34). Kessenbrock K; Plaks V; Werb Z Matrix Metalloproteinases: Regulators of the Tumor Microenvironment. Cell 2010, 141, 52–67. [PubMed: 20371345]

(35). Nagase H; Visse R; Murphy G Structure and Function of Matrix Metalloproteinases and TIMPs. Cardiovasc. Res 2006, 69, 562–573. [PubMed: 16405877]

(36). Larson RG In The Structure and Rheology of Complex Fluids (Topics in Chemical Engineering); Gubbins KE, Ed.; Oxford University Press, 1999.

(37). Mezger TG Applied Rheology, 1st ed.; Anton Paar GmbH, 2015.

(38). Macosko CW In Rheology: Principles, Measurements, and Applications; Cohen E, Gutoff E, Eds.; Wiley-VCH, 1994.

(39). Mours M; Winter HH Relaxation Patterns of Nearly Critical Gels. Macromolecules 1996, 29, 7221–7229.

(40). Discher DE; Jamney P; Wang Y-I Tissue Cells Feel and Respond to the Stiffness of Their Substrate. Science 2005, 310, 1139–1143. [PubMed: 16293750]

(41). Crocker JC; Grier DG Methods of Digital Video Microscopy for Colloidal Studies. J. Colloid Interface Sci 1996, 179, 298–310.

(42). Mason TG Estimating the Viscoelastic Moduli of Complex Fluids Using the Generalized Stokes-Einstein Equation. Rheol. Acta 2000, 39, 371–378.

(43). Savin T; Doyle PS Statistical and Sampling Issues When Using Multiple Particle Tracking. Phys. Rev. Lett 2007, 76, 1–15.

(44). Furst EM; Squires TM Microrheology, 1st ed.; Oxford University Press, 2017.

(45). Weihs D; Mason TG; Teitell MA Bio-microrheology: A Frontier in Microrheology. Biophys. J 2006, 91, 4296–4305. [PubMed: 16963507]

(46). Tseng Y; Kole TP; Wirtz D Micromechanical Mapping of Live Cells by Multiple-particle-tracking Microrheology. Biophys. J 2002, 83, 3162–3176. [PubMed: 12496086]

(47). Daviran M; Caram HS; Schultz KM Role of Cell-Mediated Enzymatic Degradation and Cytoskeletal Tension on Dynamic Changes in the Rheology of the Pericellular Region Prior to Human Mesenchymal Stem Cell Motility. ACS Biomater. Sci. Eng 2018, 4, 468–472. [PubMed: 29862316]

(48). Daviran M; Longwill SM; Casella JF; Schultz KM Rheological Characterization of Dynamic Remodeling of the Pericellular Region by Human Mesenchymal Stem Cell-secreted Enzymes in Well-defined Synthetic Hydrogel Scaffolds. Soft Matter 2018, 14, 3078–3089. [PubMed: 29667686]

(49). Salinas C; Anseth K Mesenchymal Stem Cells for Craniofacial Tissue Regeneration: Designing Hydrogel Delivery Vehicles. J. Dent. Res 2009, 88, 681–692. [PubMed: 19734453]

(50). Dikovsky D; Bianco-Peled H; Seliktar D Defining the Role of Matrix Compliance and Proteolysis in Three-Dimensional Cell Spreading and Remodeling. Biophys. J 2008, 94, 2914–2925. [PubMed: 18178662]

(51). Liu Z; Tan JL; Cohen DM; Yang MT; Sniadecki NJ; Ruiz SA; Nelson CM; Chen CS Mechanical Tugging Force Regulates the Size of Cell-cell Junctions. Proc. Natl. Acad. Sci. U. S. A 2010, 107, 9944–9949. [PubMed: 20463286]

(52). Janmey PA; Weitz DA Dealing with Mechanics: Mechanisms of Force Transduction in Cells. Trends Biochem. Sci 2004, 29, 364–370. [PubMed: 15236744]

(53). Loh XJ; Tan KK; Li X; Li J The in Vitro Hydrolysis of Poly(ester ure thane)s Consisting of Poly[(R)-3-hydroxybutyrate] and Poly(ethylene glycol). Biomaterials 2006, 27, 1841–1850. [PubMed: 16305807]

(54). Schultz KM; Baldwin AD; Kiick KL; Furst EM Measuring the Modulus and Reverse Percolation Transition of a Degrading Hydrogel. ACS Macro Lett 2012, 1, 706–708. [PubMed: 23413411]

(55). Schweller RM; Wu ZJ; Klitzman B; West JL Stiffness of Protease Sensitive and Cell Adhesive PEG Hydrogels Promotes Neovascularization In Vivo. Ann. Biomed. Eng 2017, 45, 1387–1398. [PubMed: 28361182]

(56). Navarro-Requena C; Weaver JD; Clark AY; Clift DA; Peŕez-Amodio S; Castaño Ó; Zhou DW; García AJ; Engel E PEG Hydrogel Containing Calcium-releasing Particles and Mesenchymal Stromal Cells Promote Vessel Maturation. Acta Biomater 2018, 67, 53–65. [PubMed: 29246650]

(57). Rodrigues M; Griffith LG; Wells A Growth Factor Regulation of Proliferation and Survival of Multipotential Stromal Cells. Stem Cell Res. Ther 2010, 1, 32–44. [PubMed: 20977782]

(58). Reese JS; Solchaga LA; Lingas KT; Lazarus HM; Gerson SL Improved Culture Expansion of Human Mesenchymal Stem Cells (MSCs) Using Fibroblastic Growth Factor-2 for the Treatment of Graft Versus Host Disease (GVHD). blood 2007, 110, 1207. [PubMed: 17513617]

(59). Fairbanks BD; Schwartz MP; Bowman CN; Anseth KS Photoinitiated Poly-merization of PEG-diacrylate with Lithium Phenyl-2,4,6-trimethylbenzoylphosphinate: Polymerization Rate and Cytocompatibility. Biomaterials 2009, 30, 6702–6707. [PubMed: 19783300]

(60). Zalipsky S Functionalized Poly(ethylene glycol) for Preparation of BiologicallyRelevant Conjugates. Bioconjugate Chem 1995, 6, 150–165.

(61). Sigma-Aldrich. Product Information for Collagenase from Clostrdium Histolyticum; 2012.

(62). Live/Dead Viability/Cytotoxicity Kit, for mammalian cells https://www.thermofisher.com/order/catalog/product/l3224.

(63). Metters AT; Bowman CN; Anseth KS A Statistical Kinetic Model for the Bulk Degradation of PLA-b-PEG-b-PLA Hydrogel Networks. J. Phys. Chem. B 2000, 104, 7043–7049.

(64). Metters A; Hubbell J Network Formation and Degradation Behavior of Hydrogels Formed by Michael-Type Addition Reactions. Biomacromolecules 2005, 6, 290–301. [PubMed: 15638532]

(65). West JL; Hubbell JA Polymeric Biomaterials with Degradation Sites for Proteases Involved in Cell Migration. Macromolecules 1999, 32, 241–244.

(66). Mann BK; Gobin AS; Tsai AT; Schmedlen RH; West JL Smooth Muscle Cell Growth in Photopolymerized Hydrogels with Cell Adhesive and Proteolytically Degradable Domains: Synthetic ECM Analogs for Tissue Engineering. Biomaterials 2001, 22, 3045–3051. [PubMed: 11575479]

(67). Ohbayashi N; Yamagata N; Goto M; Watanabe K; Yamagata Y; Murayama K Enhancement of the Structural Stability of Full-Length Clostridial Collagenase by Calcium Ions. Appl. Environ. Microbiol 2012, 78, 5839. [PubMed: 22685155]

(68). Tunnat A; Behr P; Gorner K Desorption Kinetics of CO2 from Water and Aqueous Amine Solutions. Energy Procedia 2014, 51, 197–206.

(69). Rubinstein M; Colby RH Polymer physics; Oxford University Press, 2003.

(70). Endres M; Kneitz S; Orth MF; Perera RK; Zernecke A; Butt E Regulation of Matrix Metalloproteinases (MMPs) Expression and Secretion in MDA-MB-231 Breast Cancer Cells by LIM and SH3 Protein 1 (LASP1). Oncotarget 2016, 7, 64244–64259. [PubMed: 27588391]

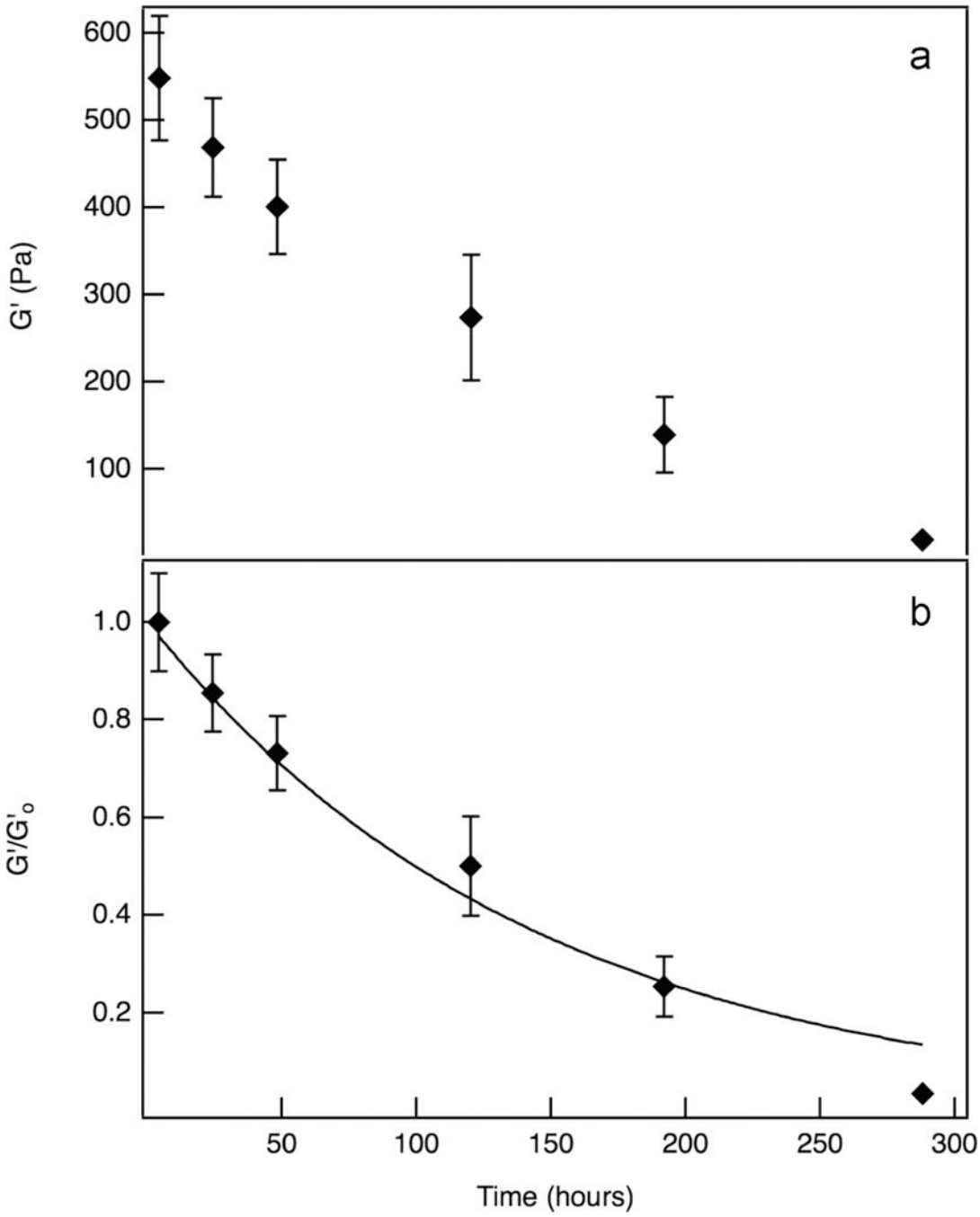

Figure 1.

Hydrolysis of PEG-norbornene hydrogel scaffolds without hMSCs. (a) Bulk rheological measurements of the elastic moduli, G', as a function of time throughout degradation. (b) Normalized elastic moduli, G'/G'_0, as a function of time. This data is fit to eq 2, resulting in a hydrolysis kinetic constant, $k_h = 7.5 \times 10^{-3} \pm 7.1 \times 10^{-4}\ h^{-1}$.

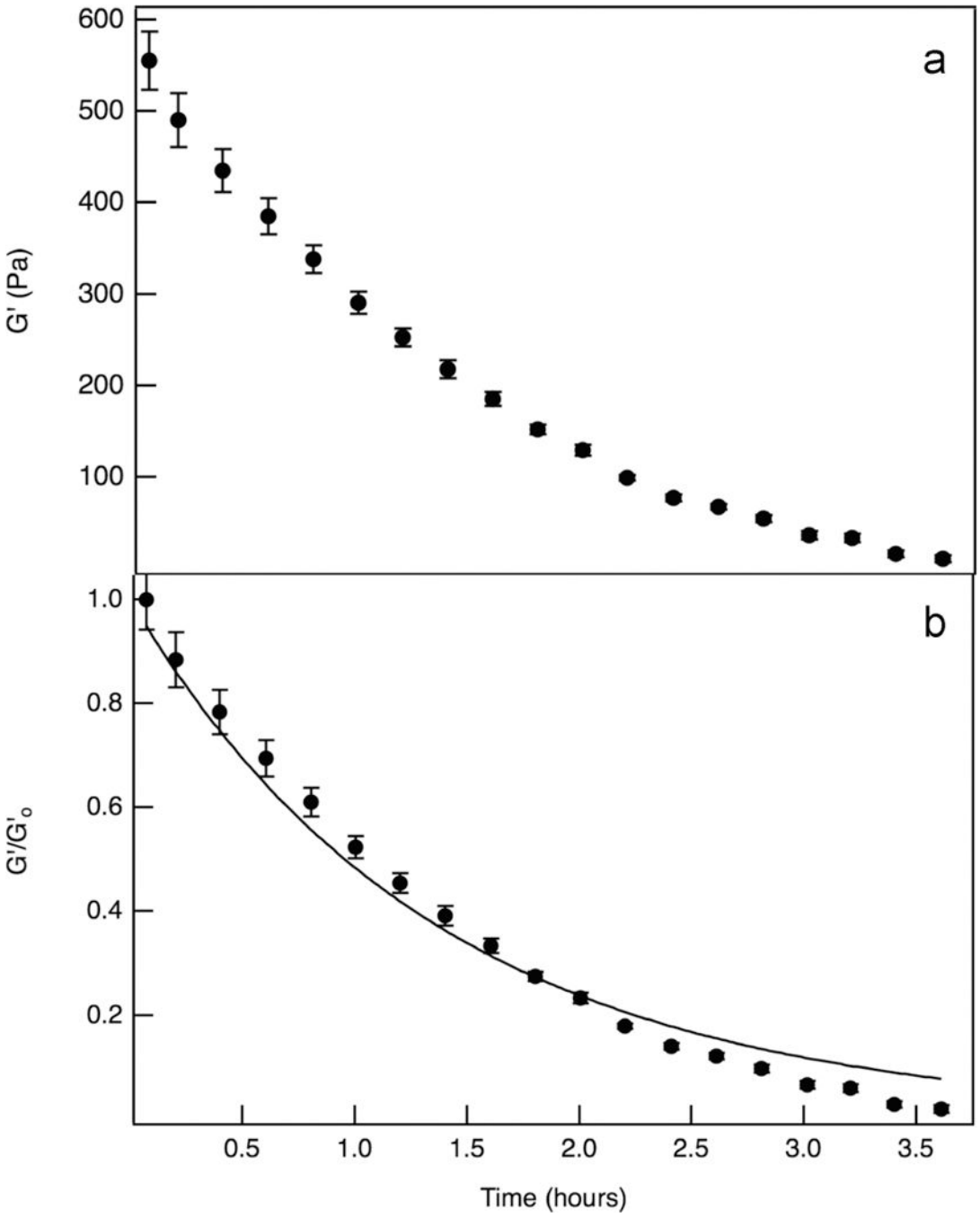

Figure 2.

Noncellular enzymatic degradation, initiated by immersing hydrogels without hMSCs in a 0.3 mg/mL collagenase solution. (a) Bulk rheology measures the elastic moduli, G', as a function of time. (b) Normalized elastic moduli, G'/G'_0, as a function of time. Enzymatic degradation is modeled using eq 3, resulting in an enzymatic kinetic constant, k^* = 86.7 ± 0.71 M^{-1} s^{-1}.

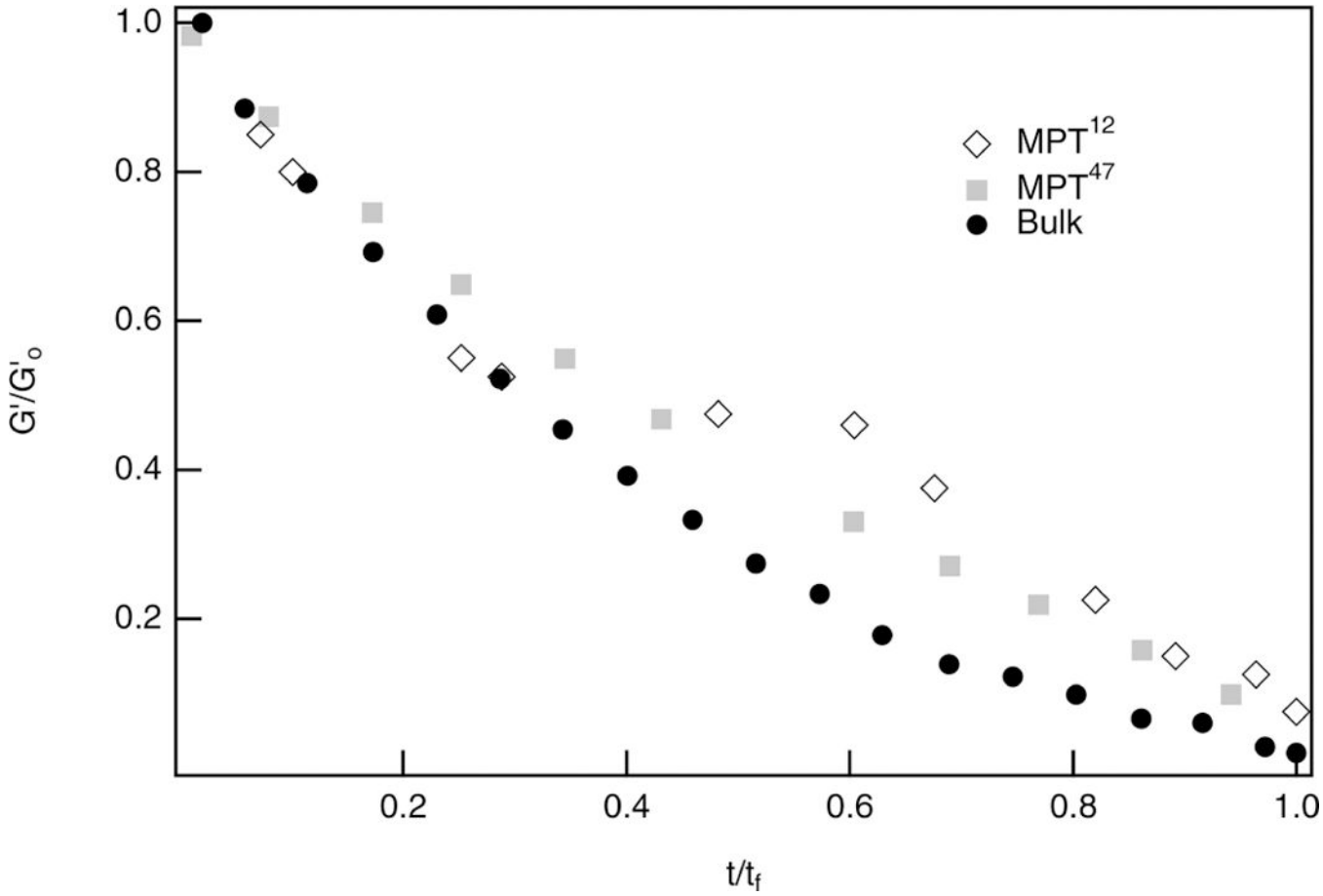

Figure 3.

Normalized elastic moduli, G'/G'_0, measured with bulk rheology and multiple particle tracking microrheology, showing comparability between the characterization techniques over the entire noncellular enzymatic degradation reaction.[12,47]

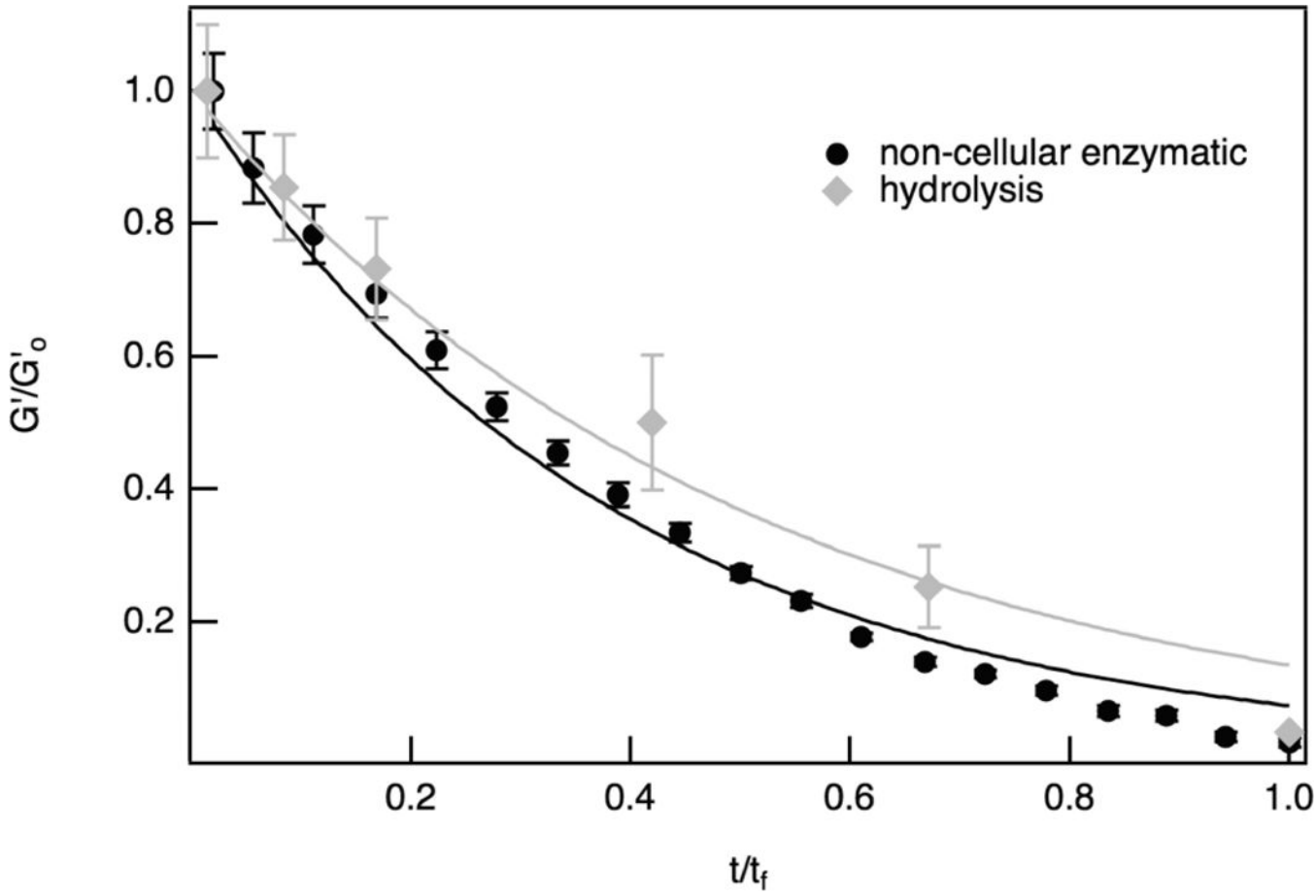

Figure 4.
Bulk rheology results for hydrogels without encapsulated hMSCs, comparing hydrolysis and noncellular enzymatic degradation.

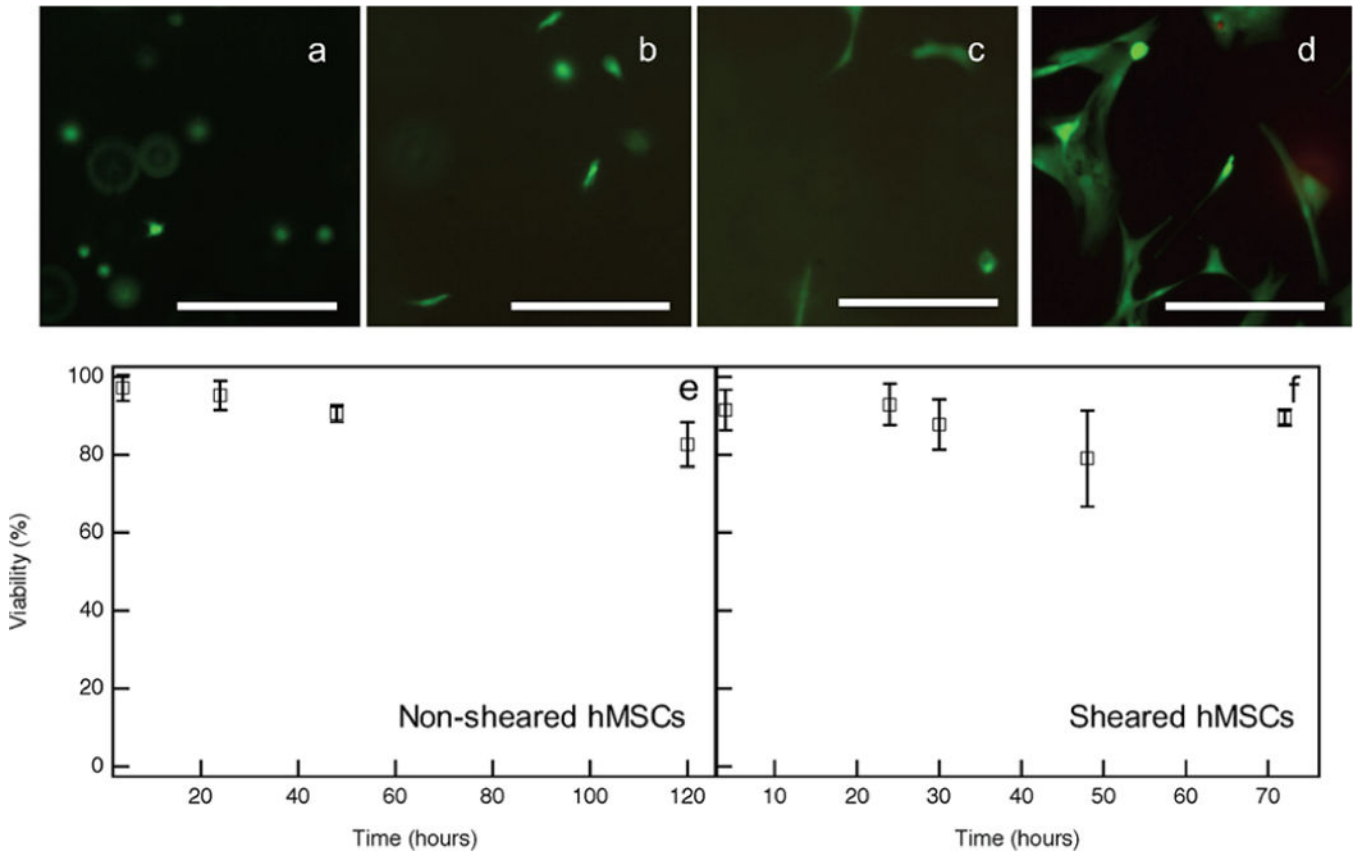

Figure 5.

Incubation viability for hydrogels with encapsulated hMSCs quantified using a Live/Dead Assay. Fluorescent images of live hMSCs at (a) 4, (b) 24, (c) 48 and (d) 120 h after hMSC encapsulation. Data and images show a high viability and increased motility with time. Scale bars are 250 μm. hMSC viability as a function of time (shown as percent of viable cells) for (e) non-sheared and (f) sheared hMSCs.

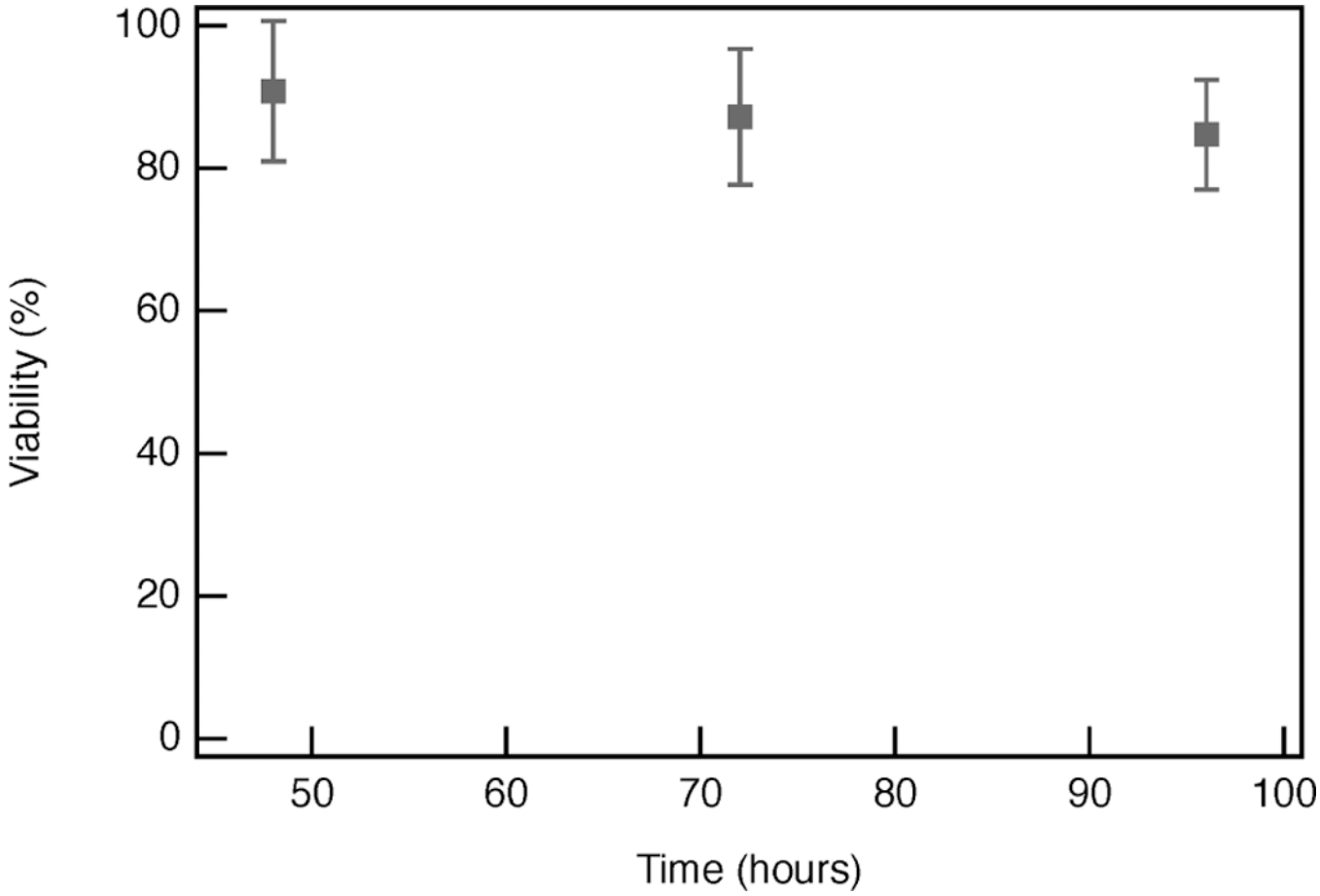

Figure 6.
hMSC viability as a function of time at 0, 24, and 48 h of incubation following shearing on the rheometer. Note that, for each of these experiments, shearing is completed 48 h after hydrogel formation, so viability is completed on hydrogels at 48, 72, and 96 h, respectively, in real time.

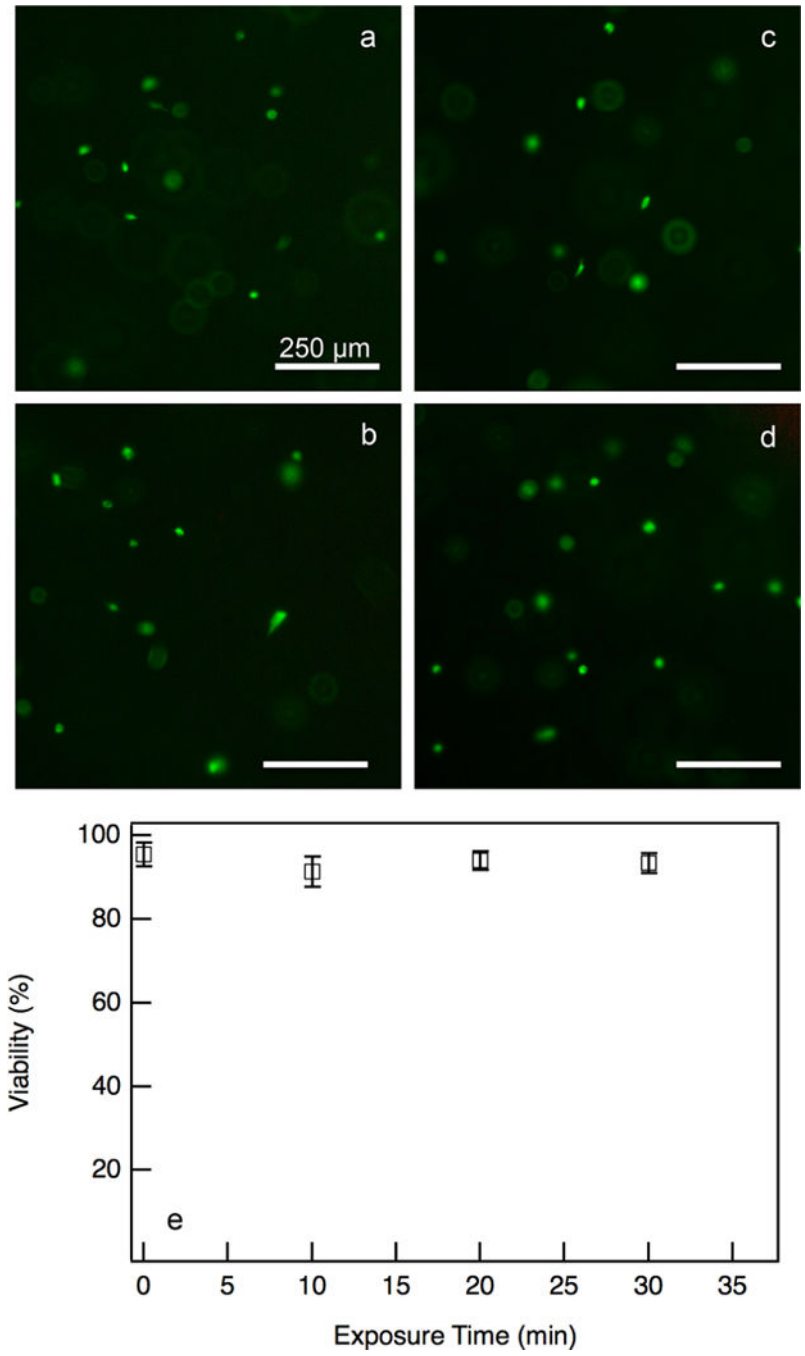

Figure 7.

Exposure viability of hydrogels with encapsulated hMSCs exposed to atmospheric conditions without growth medium for 0–30 min. Fluorescent images of live cells at (a) 0, (b) 10, (c) 20, and (d) 30 min. (e) Quantification of percent viability over the same time period. There is no significant change in viability over 30 min, indicating this exposure does not cause significant cell death.

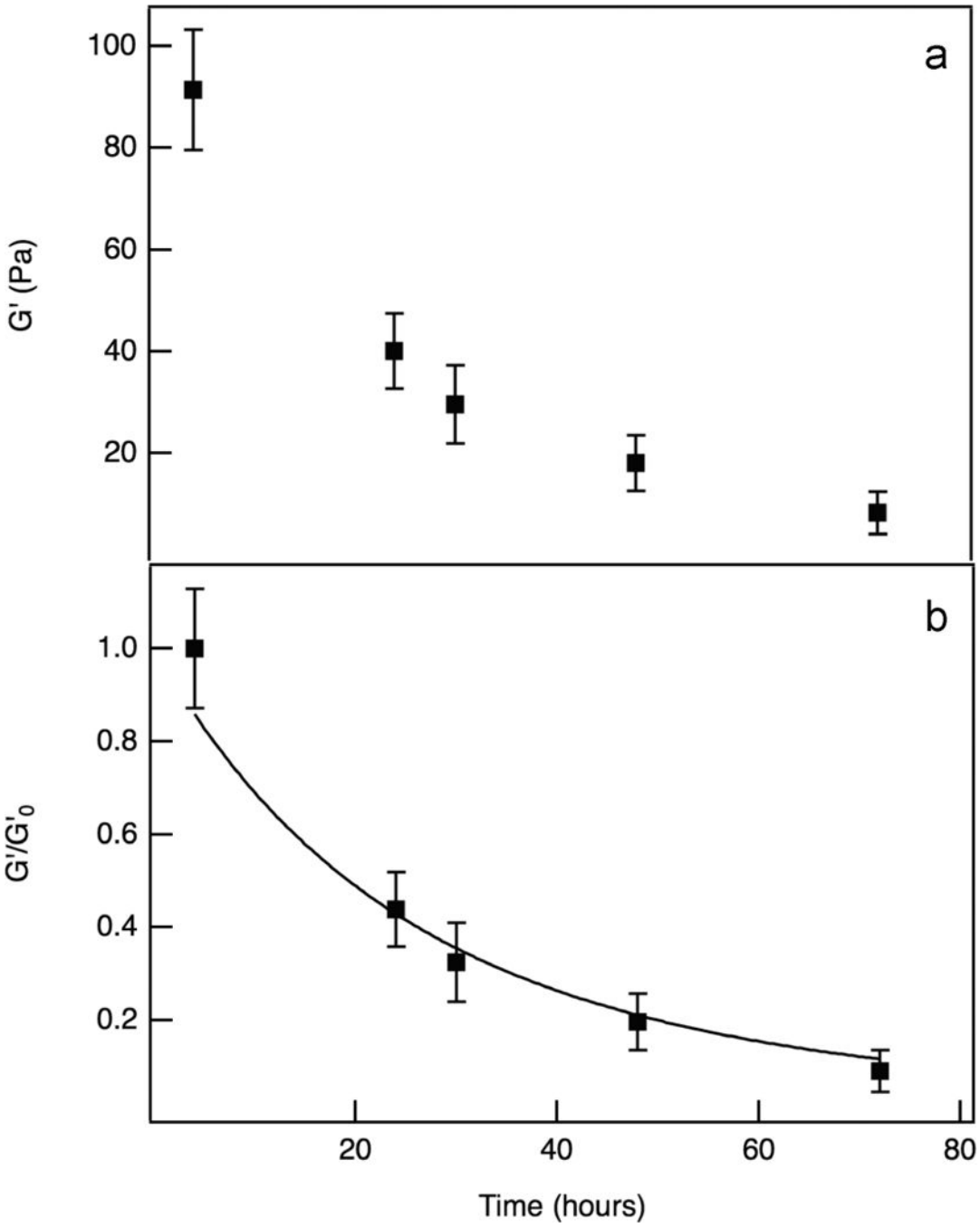

Figure 8.

Cell-mediated enzymatic degradation. (a) Elastic moduli, G', as a function of time, characterized with bulk rheology throughout the degradation reaction. (b) Normalized elastic moduli, G'/G'_0 as a function of time. This data is fit to eq 4, where k_d and k^* are the first-order rate and enzymatic kinetic constants, respectively. This fit resulted in an initial MMP concentration, [MMP_0], of $1.23 \times 10^{-7} \pm 1.35 \times 10^{-8}$ M for a hMSC encapsulation concentration of 2×10^5 cells/mL.

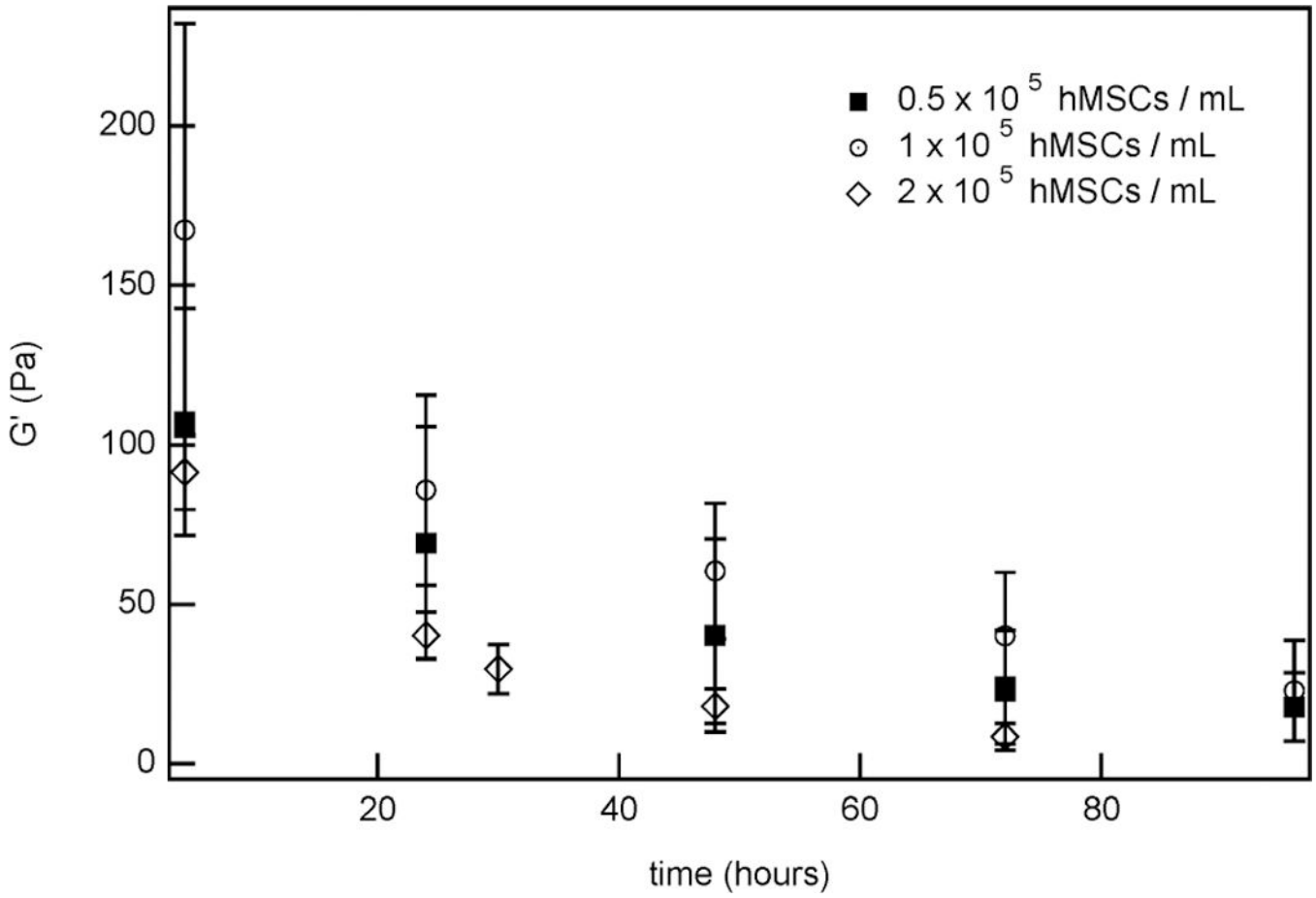

Figure 9.
Measurements of hydrogel moduli over time for different initial hMSC concentrations.

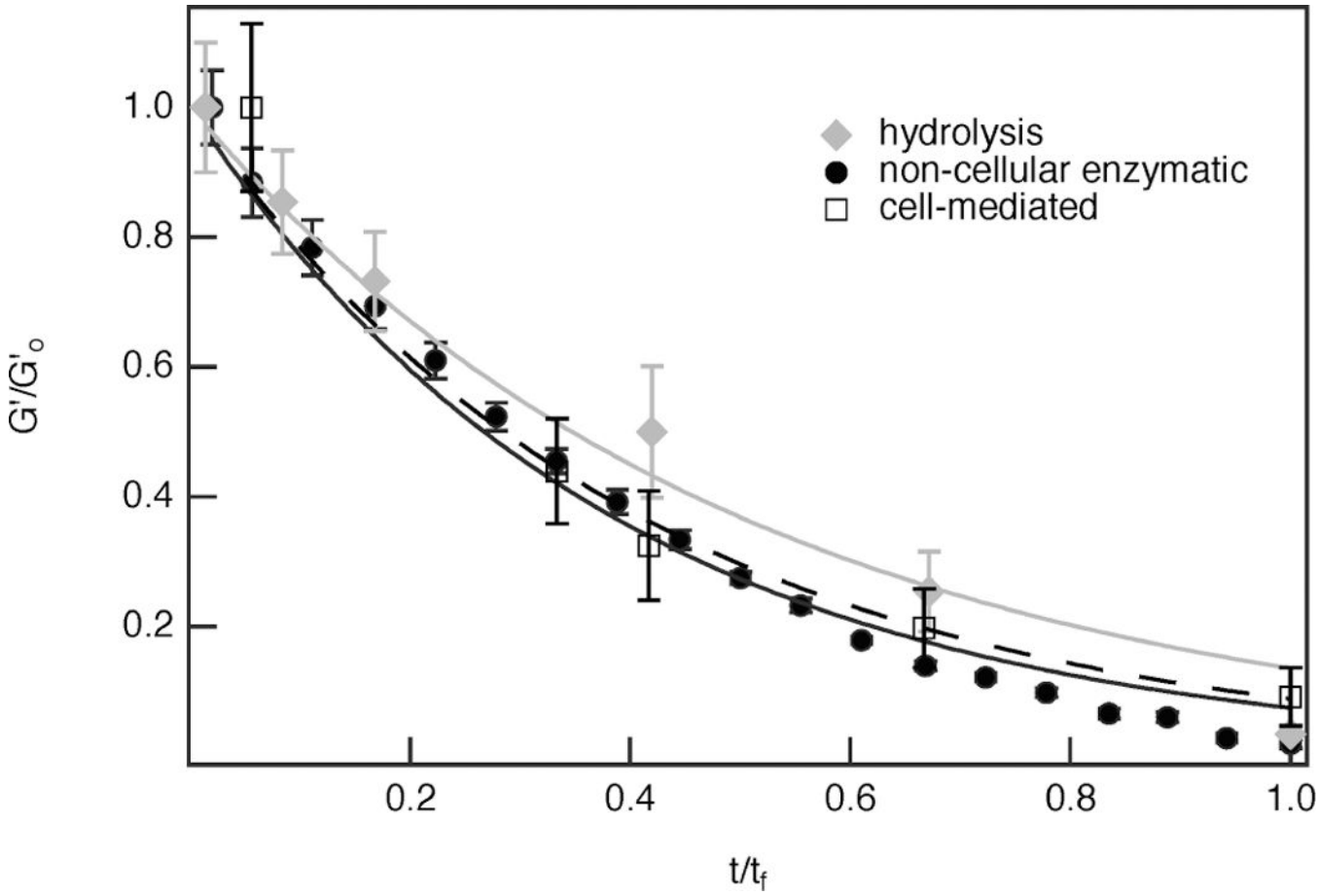

Figure 10.
Comparison of hydrolytic (gray line), noncellular enzymatic (black, solid line), and cell-mediated (dashed line) scaffold degradation. The initial hMSC concentration in the cell-mediated degradation experiment is 2×10^5 cells/mL.

Table 1.

Measured Modulus and Calculated Cross-Link Density for Swollen Hydrogels from Bulk Rheology Experiments

experiments	G' (Pa)	$\rho\,(m^{-3})$
swollen hydrogel without hMSCs	550	1.34×10^{23}
swollen hydrogel with hMSCs	100	2.43×10^{22}
ideal system with 100% cross-link form		4.70×10^{23}